Novel V2G Regulation Scheme Using Dual-PSS for PV Islanded Microgrid

Abubakr, Hussein; Lashab, Abderezak; Vasquez, Juan C.; Mohamed, Tarek Hassan; Guerrero, Josep M.

Published in:
Applied Energy

DOI (link to publication from Publisher):
10.1016/j.apenergy.2023.121012

Publication date:
2023

Document Version
Publisher's PDF, also known as Version of record

Applied Energy 340 (2023) 121012

Contents lists available at ScienceDirect

Applied Energy

journal homepage: www.elsevier.com/locate/apenergy

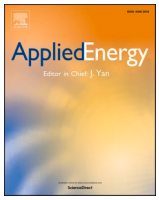

Novel V2G regulation scheme using Dual-PSS for PV islanded microgrid

Hussein Abubakr [a,b,*], Abderezak Lashab [a], Juan C. Vasquez [a], Tarek Hassan Mohamed [b], Josep M. Guerrero [a]

[a] Center for Research on Microgrids (CROM), AAU Energy, Aalborg University, 9220 Aalborg, Denmark
[b] Department of Electrical Engineering, Faculty of Energy Engineering, Aswan University, Aswan 81528, Egypt

HIGHLIGHTS

- Adaptive PID-PSS of V2G for frequency, voltage, and power-sharing regulations.
- PSS device for V2G grid regulation side along with the generation side.
- Transient stability performance of a solar PV-powered MG.
- A complementary signal to promote faster oscillatory V2G regulation instability.
- Improved regulatory capability during EV's charging and regulation periods.

ARTICLE INFO

Keywords:
Vehicle-to-grid
Power system stabilizer
Residential microgrid
Solar photovoltaic
Power sharing
Adaptive control

ABSTRACT

The incorporation of electric vehicles (EVs) into residential/industrial microgrids (MGs) presents some limitations such as fluctuations in voltage, frequency, and lack of power supply. According to the literature, the control methods for vehicle-to-grid (V2G) in MGs are insufficiently coordinated for charging and regulation, limited by narrow charging control constraints, complex, and computationally demanding. Moreover, the power system stabilizer (PSS) is employed only in the generation side. To this regard, a PSS is proposed in this paper along with the proportional-integral-derivative (PID) controller, which is tuned adaptively using Harris hawks optimizer (HHO) for frequency, voltage, and power-sharing regulations through the parked EVs. The considered islanded MG is consisting of a diesel generator as a backup generation source, dealing with the intermittent nature of the solar photovoltaic (PV) plant and residential load. It also includes an EV aggregator. In case of partial shading of the solar PV farm and triggering the load demand, the proposed control strategy provides a complementary signal to promote short response time during transients, boost the transient stability performance, and offer damping characteristics adequate for V2G regulation with the islanded residential MG. To examine the efficacy of the proposed scheme, a detailed simulation model using Matlab/Simulink was built. The final findings show that the proposed direct adaptive PID-PSS controller gives significantly enhanced voltage and frequency with spinning reserve compared to the conventional PI-controller both considering the inclusion of V2G on the MG regulation side and conventional controller without V2G and PSS on the regulation side. Also, it can provide power flow in a bi-directional way during the partial shading contingency that the residential MG may experience within 24 hr.

1. Introduction

Nowadays, the escalation of environmental problems such as the depletion of non-renewable energy sources (RESs) and emission of CO_2, mostly caused by transport and industry sectors have jutted out. These conditions alert all communities to discover sustainable solutions in this matter. In this context, the inception of electric vehicles (EVs) has become globally promising for domestic and industrial transportation since it is an applicable solution to alleviate the issues caused by conventional internal combustion (IC) vehicles [1]. In addition, EVs have been presenting great support due to their multiple benefits that make the ownership of EVs increases such as no environmental pollution (no emit CO_2), energy efficiency and security, power saving, smooth operation, and significantly low vibration and noise due to less motion part included in EVs [2].

* Corresponding author at: Center for Research on Microgrids (CROM), AAU Energy, Aalborg University, 9220 Aalborg, Denmark.
E-mail address: haha@energy.aau.dk (H. Abubakr).

https://doi.org/10.1016/j.apenergy.2023.121012
Received 4 November 2022; Received in revised form 18 February 2023; Accepted 19 March 2023

Nomenclature

Indexes

Δf	MG frequency deviations (Hz)
$\Delta\omega_r$	Change in rotor speed (rad/s pu)
ΔE_i	The ith EV battery energy variation
ΔP_m	Mechanical power variation (MW pu)
P_{eo}	Output electrical power from diesel (MW pu)
P_L	Demand load power (MW)
P_{PV}	Solar PV power (MW)
P_{chg}	V2G charging power (MW)
Q_{chg}	V2G charging reactive power (MVAR)
P_{reg}	V2G regulation power (MW)
Q_{reg}	V2G regulation reactive power (MVAR)
Q_{eo}	Output reactive power from synchronous machine (MVAR pu)
Q_{PV}	Solar PV reactive power (MVAR)
Q_L	Demand load reactive power (MVAR)
V_{PSS}	Power system stabilizer voltage (V)
V_L	Demand load terminal voltage (V)
V_{PV}	Solar PV terminal voltage (V)
V_f	Excitation field voltage (V)
I_L	Demand load current (A)
I_{PV}	Solar PV current (A)
$P_{j,k+1}^{up,1}$	Up regulation V2G power of the jth charging station at time k + 1
$P_{j,k+1}^{down,1}$	Down regulation V2G power of the jth charging station at time k + 1
SOC_i^{max}	Maximum SOC of the ith EV
SOC_i^{min}	Minimum SOC of the ith EV
$SOC_{i,k}$	SOC of the ith EV at time k
SOC_i^{in}	Initial SOC of the ith EV at plug-in time
$K_{i,k}^{up}$	Up regulation factor
$K_{i,k}^{down}$	Down regulation factor
P_{max}	Maximum V2G power (MW)
$P_{i,k+1}$	V2G power at battery side of ith EV at time k + 1
R_S	Series resistance (Ω)
R_t	Shunt resistance (Ω)
C_t	Shunt capacitor (μF)
η^C	EVs charging efficiency
η^d	EVs discharging efficiency
ω	Rotor speed (rad/sec)
K_{PSS}	Stabilizer gain
K_P	Proportional gain
K_i	Integral gain
K_D	Derivative gain
K_r	Regulation gain
K_A	Amplifier gain
K_E	Exciter gain
$K_1 - K_6$	Coefficient parameters in real output power
D	MG damping coefficient (pu MW/Hz)
M	Equivalent inertia constant (pu sec)
E_i^r	The ith EV battery rated capacity
T_E	Exciter time constant (sec)
T_A	Amplifier time constant for exciter in (sec)
T_r	Regulator time constant for V2G regulation side (sec)
T_w	Washout time constant in (sec)
T_s	Settling time (sec)
M_P	Maximum overshoot
e_{ss}	Steady state error
ω_n	Natural frequency
ζ	Damping ratio

Acronyms

EV	Electric Vehicle
V2G	Vehicle-to-Grid
G2V	Grid-to-Vehicle
MG	Microgrid
PV	Photovoltaic
PSS	Power System Stabilizer
SOC	State of Charge
DG	Distributed Generator
WECC	Western Electricity Coordinating Council Standard

Several countries located in Europe embolden their people to use EVs with various regulations. For example, Denmark and Norway are leading the race in using this technology and Netherlands is joining them in debating whether to ban gas and diesel-powered vehicles by 2025 [3].

Renewable energy sources (RESs) such as wind farms and solar photovoltaic (PV) parks can be utilized to generate electricity without any greenhouse gas emissions (GHGs) and can be used sustainably for charging EVs to eliminate grid-related impacts and indirect GHG emissions from EVs. However, the major drawback to this technology is the intermittent and unpredictable nature of RESs. Also. RESs require a backup system to support them in various operating conditions and convert the irregular power to a uniform one. One of the potential alternatives is to implement the vehicle-to-grid (V2G) scheme [4].

1.1. Literature survey

Several scholars have stated that EV technologies have a benefit in facilitating their enforcement and guaranteeing an eco-friendly environment on top of the conventional energy-provision ones. As a result, from [4–6], an inclusive classification has been comprehensively shown on the basis of the inclusion of EVs and their methodologies in order to detect possible gaps and indicate the direction of future studies toward feasibility, aggregation, social, technical, and regulatory aspects and challenges.

In [7,8], different applications have been used for EVs, where the most important is the inclusion of V2G that is used for frequency and power regulations, from which the idea of V2G gives useful means of interactions between EVs and microgrids (MGs), with EVs treated as distributed generators (DGs) that can supplement the grid resulting in higher stability. In [9], A virtual energy storage system based on the EV frequency control strategy is proposed for enhancing the EV user's traveling behavior, without considering the study of demand response-based controllable loads. The V2G feature can assist in stabilizing the voltage, shifting the peak load, spinning reserve, assuaging rapid spikes of the grid loads, and frequency regulation. From the author's point of view, with V2G in demand, vehicles authorize power to be supplied to other elements of the MG in high-demand periods and thus can store energy in the excess power of RESs and recognize it promptly. In [10,11], comprehensive reviews of various V2G systems are presented, which illustrate the V2G impacts on the utility interfaces and distribution systems supported by negative and positive commands during charging EVs. In [4,12–16], researchers have done several works to analyze the effectiveness of V2G in surpassing problems caused by the penetration of intermittent RESs and how these sources will affect the primary frequency regulation in industrial and residential MGs. In [17], a smart EV charging technology-based solar PV with the inclusion of V2G to support the grid has been presented to achieve satisfactory operation and mitigate the power fluctuations in PV. Furthermore, the

design of a PV-integrated EV charging system was discussed with the multifunctional operational capability to coordinate various sources in the system [18]. Several challenges during the EVs incorporation into the MG such as absorption of high energy, increased peak demand, and issues of power quality (i.e. harmonics), as well as the unpredictability of the dynamic behaviors, are reviewed in [19].

Frequency regulation is a critical challenge in MGs to overcome. Therefore, numerous works have been made on MGs frequency regulation. In [20], the feasibility and available capacity of EVs for frequency regulation was estimated in a probabilistic manner to find out how much the achievable power capacity could be provided to the grid operator by V2G aggregators. In [21], a new coordination strategy for frequency regulation in multi-areas is introduced by online tunning the integral controller gains using Harris hawks optimizer (HHO) to charge/discharge EVs considering solar PV. The control method supported also the virtual inertia mechanism as an auxiliary control loop. In [22] a new V2G strategy to control the primary frequency is proposed for industrial MGs, involving effective coordination of the charging station operator, EV aggregator, and EV operator. In addition, a built-in droop control method was presented to enhance the performance of primary frequency control [23]. In [24], an adaptive droop control strategy has been suggested to control the EV battery discharging/charging process using a hierarchical game theoretical method for energy management. Also, a smart droop control for simultaneous regulation of voltage and frequency in islanded and smart MGs for load change behaviors was developed in [25]. The concept of direct adaptive control was investigated in [26,27] to adjust the parameters of the primary and secondary controllers. In [26], the electro-search optimizer has been proposed for load frequency control (LFC) to regulate the power and frequency considering nonlinearities, such as governor dead bands and generation rate constraints. In [27], a new coordination scheme for multi-area MGs using a modified virtual rotor mechanism supported with balloon effect modulation (BE) was proposed. In [28], the income associated with EVs involvement in V2G frequency regulation was presented by implementing uncertain dispatch in the control center without projecting state of charge (SOC) levels for EV batteries.

Power system stabilizer (PSS) has been studied in many works, which are focused only on the generation side through the excitation system to deliver suitable damping properties for the synchronous generators (SGs) such as in [29,30]. Furthermore, several types of PSS such as the standard Lead-Lag PSS, PSS2A-based WECC standard method (WECC is the Western Electricity Coordinating Council), and type 2A-PSS-based soft optimizers have been discussed for different power system applications in [30–32].

1.2. Motivation and challenges

EVs can act as loads in normal operation (charging) and sources in abnormal conditions (regulation) called controllable loads/mobile storage devices. Although incorporating EVs into MGs has a positive significance in enhancing the reliability and stability during peak loads as explained in the literature part, this may present some constraints in the grid such as fluctuations in voltage, frequency, and lack of power supply. Therefore, the effectiveness of the MG will also be particularly affected at the moment of peak demand due to the high power required during the charging process time by the owners.

Basically, there are two states for demand, as follows. First, during the on-peak period when demand is high, fluctuations within the grid increase, so it is necessary to add auxiliary SGs to reduce them, and this is a more expensive solution. Second, during the off-peak period (nighttime) when demand is low, unused power generated from additional sources can be wasted. Thus, the idea of V2G inclusion was created in order to solve these hurdles in the grid by providing an additional demand/supply balance service that can be utilized in three ways: spinning and non-spinning reserves, and regulation up and down. Based on the previous observation, few works have been made to contrive the EVs regulation and to attempt the ability of power-sharing, frequency, and voltage regulations. For the fluctuations, in fact there is no evidence that they will occur during peak loads because they can occur at any time during the day. Therefore, in this work, we considered the peak load as the worst scenario for the study because the power consumption is high compared to other day-periods and more energy needed to cover the peak loads.

As reported in the literature, up/down regulation response has been achieved with higher time. In addition to the complexity of the control schemes that were used for adjusting the system's parameters with more needed time for computations. Furthermore, the PSS controller has been utilized in the power system only the generation side to reduce the oscillations in the MG terminal voltage while neglecting the MG regulation side aspect.

1.3. Paper contributions and organization

This research set out to define the V2G role in controlling the primary frequency and terminal voltage by providing improved properties for damping to reset the output steady-state offset. The main features and contributions of this study can be outlined as follows:

i. A novel control scheme based on the direct adaptive PID-PSS in the case of V2G is introduced for primary frequency and power-sharing regulations.
ii. The PSS device is added for the first time on the MG regulation side along with the generation side to offer appropriate damping characteristics for the V2G regulation and to boost the transient stability performance of a PV-powered MG.
iii. The addition of PSS with output boundaries can reduce the fluctuation degree of the terminal voltage through transient situations, thereby enhancing the dynamic stability performance of the studied MG system.
iv. A complementary signal is demonstrated to promote faster oscillatory instability on the V2G microgrid regulation side.
v. A high regulatory capability is achieved by coordinating the EV's charging and regulation periods by EV aggregators using the proposed scheme.
vi. The proposed control strategy can effectively accord with system uncertainties such as sudden load disconnection and partial shading of the solar PV plant.

The rest of this work is outlined as follows: Section 2 introduces the main ancillary services provided by EVs. The main configuration of the proposed islanded residential PV-based MG is defined in Section 3. In Section 4, the proposed control scheme for MG regulation is demonstrated. Section 5 shows the dynamic response simulations and discussions of the proposed control method. Section 6 concludes the work.

2. EV as an ancillary service in the grid

Electric vehicles are the widest spreading technology worldwide, not only because they reduce the reliance on conventional sources of energy but also play a key role in decreasing the emission of hazardous elements into the environment and achieving a low-carbon future.

Services provided by EVs to the grid can be a spinning reserve, congestion management, regulating the power factors, peak shaving, and voltage and frequency control. For normal situations, the system operates at nominal frequency, maintaining an equal state between demand and generated power. Several issues occur in MGs due to an imbalance between the load and generating power, followed by oscillations leading to frequency and voltage deviations, which if not controlled early will result in a power outage. In order to maintain the state of power balance, the system operator should offer various services purchased from the generating units in the market. Table 1 states the V2G feasibility in supporting various system services [33].

Table 1
Various electricity market characteristics [33].

Service	Base load	Peak power	Spinning reserve	Regulation
Description	Constant part of demand for power	Fluctuation part of demand power	Quick power for grid failures	Power for voltage and frequency stabilization
Utilization frequency	–	Once/day	Low	High
Utilization time	24 hr/day	2–3 hr/day	Short	Very short
Cost	Low	Moderate	High	High
General facility	Bulk power plant	Engine/gas turbine	Quick power generator	Battery/ Capacitor
V2G feasibility	Bad	Very good	Very good	Good

Fig. 1 displays the use of V2G encapsulation at various times of the day. A similar concept is demonstrated in [34]. There are three periods for charging and regulating the EV units: the first is daytime, in this time the solar PV can be connected to charge the EV and feed the house. The second is evening time. If an abrupt event occurs, where the amount of power generated from solar becomes less than the demanded one, EVs can help carry the peak loads and regulate the frequency to keep the grid stable. The third scenario is during nighttime, which is called 'Off-Peak', where low-cost power can be supplied by the grid to charge the car. During high energy demand, EVs can provide power back to the grid to help stabilize energy consumption by acting as personal power stations, as shown in Fig. 1. The power flow is depicted by a black arrow.

3. System configuration

3.1. Solar PV model

In this study, the solar PV farm is directly connected to the residential MG using an average model as shown in Fig. 2. Fig. 2 shows the process of converting the solar irradiance profile into a current, which is divided on the voltage difference between phases V_{ab} and V_{bc}. The two controlled current sources (CSSs) are feeding directly phase A and phase B, while Phase C is assumed to be complementary [35].

3.2. MG description

The studied MG consists of a diesel generator, solar PV plant, residential loads, and EV aggregator which are assumed to work in island mode. Solar PV plant production relies on meteorological conditions, the PV plant-covered area, and panel efficiency. The diesel generator

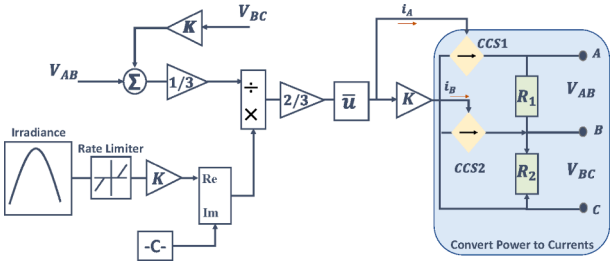

Fig. 2. Solar PV model.

acts as a reserve that poises the load consumption power on demand and the production power of the PV plant. In this study, the residential load is modeled to have a consumption pattern similar to typical household usage, and its power factor is determined based on a given profile [35].

All these sources are linked to a common bus connected through a three-phase step-down (star-star) transformer. At the transformer's secondary side, the V2G system is incorporated, and the load is delivered on the same bus. Table 2 states all sources' power capacity and load demand also the overall system of the studied islanded MG is shown in Fig. 3.

3.3. Electric vehicle model

Fig. 4 describes the schematic EV model. It is seen from Fig. 4 that the open-circuit voltage V_{SOC} is the only consideration when determining the output power of an EV (ignoring the impact of series and transient resistance on battery voltage). Then, the battery is charged and discharged by I_{ch-dis} current. The parallel RC network (R_t, C_t) describes the impacts of transient overvoltage, where (R_s) indicates the battery terminal resistance. As shown in Fig. 4, the first-order transfer function states how the charging current of the battery varies regarding frequency deviation (Δf). Also, $K_{EV}$and T_{EV}mean EV droop gain and time constant. To maintain different initial SOC levels flexibly, the adaptive droop control is taken into account with a balance SOC holder [36].

As mentioned in section 2, EVs have two main key functions, i.e. when connected to MG, the first is when acting as loads (absorb power

Table 2
Power Capacity per source.

Source	Power rating
Diesel generator	15 MW
PV plant	8 MW
EVs	4 MW
Load1	10 MW
Load 2	3 MW

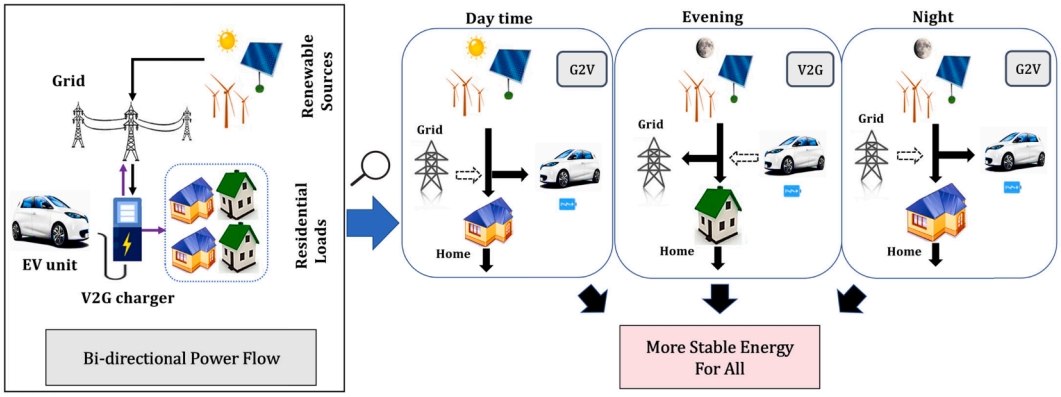

Fig. 1. The inclusion of V2G concept during different day times.

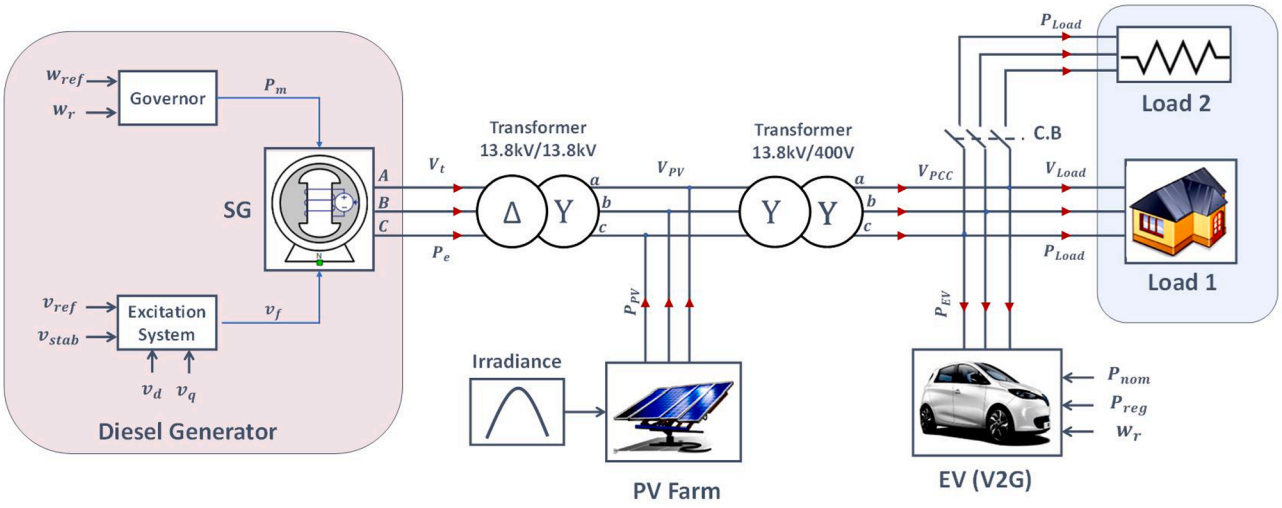

Fig. 3. Residential islanded PV-based MG configuration.

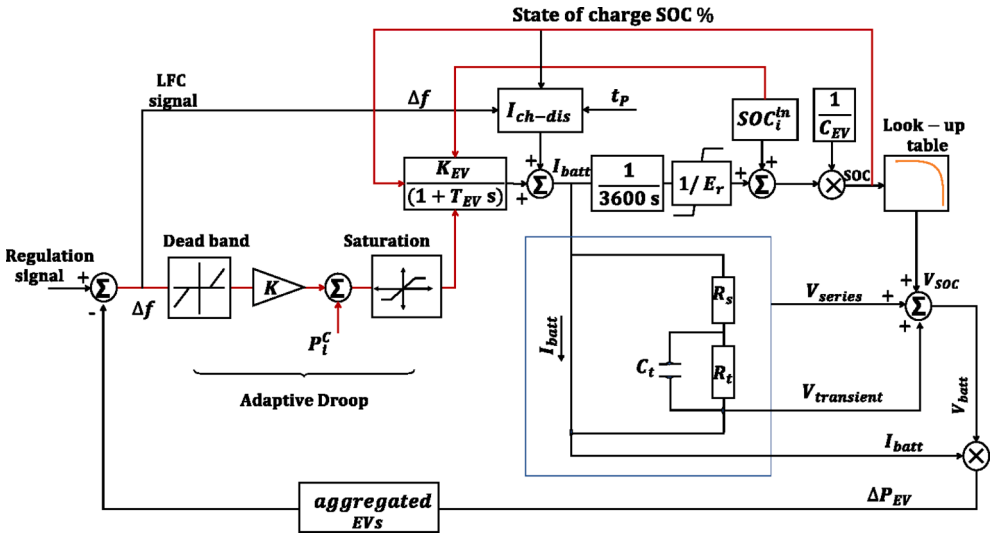

Fig. 4. EV block diagram model.

for charging or MG as a grid-to-vehicle G2V). Second, they can be used as storage units (supply power to the load or MG as V2G) to subtend the system demand and give supplementary services for regulating primary and secondary frequencies. The instant EV battery charging state is defined as follows [14]:

$$P_{EV}^{t} = P_{EV}^{max}\left(1 - e^{\left(\frac{at}{tmax}\right)}\right) + P_{EV}^{C} \tag{1}$$

where P_{EV}^{C} and P_{EV}^{max} mean the current status of the battery and maximum EV power capacity, respectively. *tmax* is the maximum time for charging, and *at* is the capacity factor at instant time *t*. Similarly, the discharging state of the EV battery is expressed as:

$$P_{EV}^{t} = P_{EV}^{C} \cdot e^{\left(\frac{at}{tmax}\right)} \tag{2}$$

For the I_{ch-dis} can be obtained by:

$$I_{ch-dis} = \frac{desired\ SOC - SOC_i^{in}}{(Plug\ in - plug\ out)\ time\ of\ EV} \times \frac{1}{E_i^r} \tag{3}$$

Where E_i^r is the ith EV battery rated capacity.

4. V2G based direct adaptive PID-PSS for microgrid regulation

4.1. Power system stabilizer

Power system stabilizer is a device that boosts the dynamic stability performance of the power system [37]. It serves as a supplementary device associated with V2G on the MG regulation side to evolve additional system stability constraints. The main objective is to improve the overall response of the considered residential MG system in terms of over/undershoot and stabilizing the system in a shorter time. This concept comes from the PSS when equipped with an excitation system to provide a stabilizing signal. Due to its powerful performance and simplicity in implementation, a PID controller is proposed in this work and tuned adaptively using HHO optimizer as presented in [30].

In this study, two PSSs are used as follows; The first is connected to the excitation system of the SG in the generation side. The second PSS is proposed inside the V2G scheme, which is connected to the MG in the regulation side. The input signal of the PSS is the deviation in rotor speed ($\Delta\omega_r$) which comes directly from the SG as shown in Fig. 5. Moreover, it comprises a regulator that acts as a high pass filter to provide suitable damping characteristics for the V2G regulation of the considered residential islanded PV-based MG system and tries to reset

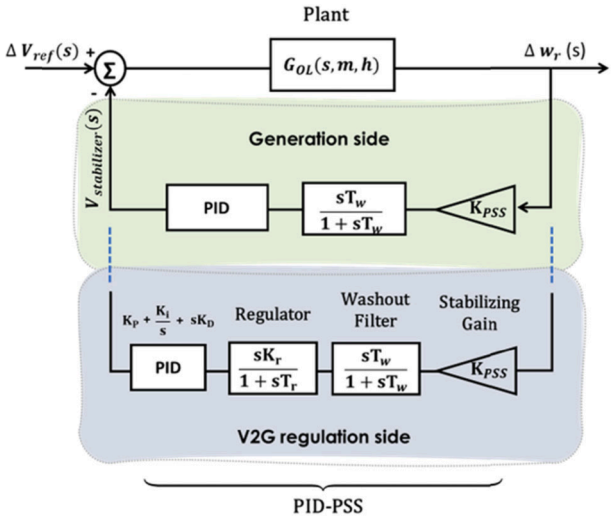

Fig. 5. Overall closed-loop transfer function-based PID-PSS structure for both generation and regulation sides.

the offset steady-state in the PSS output. Fig. 6 shows the linear synchronous machine model linked to the MG with the proposed control scheme. The configuration of the PSS device, that is linked with the excitation system and the MG regulation side, consists of (i) main regulator, (ii) PID, (iii) damping filter, (iv) stabilizing gain, and (v) output limiters. The state-space equation can be expressed as:

$$\frac{dx(t)}{dt} = Ax(t) + Bu(t) \tag{4}$$

$$y(t) = Cx(t) \tag{5}$$

$$x(t) = \left[\Delta\delta(t) \quad \Delta\omega(t) \quad \Delta E_q^{'}(t) \quad \Delta E_{fd}(t)\right]^T \tag{6}$$

where $x(t)$ is the state vector, $u(t)$ is the control input, $y(t)$ is the control output, and A, B, and C are the matrices of the appropriate dismissions. Also, the mathematical model of the proposed regulation control-based PID-PSS is given as:

$$V_{stabilizer} = \left(\frac{K_r T_w s^2}{(1+T_r s)(1+T_w s)}\left(K_P + \frac{K_i}{s} + sK_D\right)\right) \times K_{PSS}\left(\Delta\omega_{ref}(s) - \Delta\omega_{ro}(s)\right) \tag{7}$$

where K_r and K_{PSS} symbolize the regulation and stabilizer gains and K_P, K_i and K_D are the proportional, integral, and derivative controller gains, respectively. T_r and T_w indicate the regulator and washout time constants in sec.

The target in this study is to reduce the MG system response indices (i.e., Max. over/undershoot M_P, settling time T_s, and steady-state error E_{ss}). This can be achieved by obtaining a second-order system compared to the standard formula for calculating the nominal damping ratio (ζ) and natural frequency (ω_n).

The desired objective function is a function of the on-time value of $\Delta\omega_r$ and V2G regulation power (P_{reg}), and it is based on M_P, T_s, and E_{ss}. and can be identified as:

$$J_{objective} = minf\left(M_P, T_s, E_{ss}\right) \tag{8}$$

To calculate these parameters, there are two paths discussed in this work. The first one is using the Heffron-Philips's mode [38] which is simplified in Fig. 6 in open loop, as follows:

$$G_{plant}(s,m,n) = \frac{\Delta\omega_r(s)}{\Delta V_{ref}(s)} = \frac{-ms}{h_4 s^4 + h_3 s^3 + hs^2 + hs + h_0} \tag{9}$$

where,

$$\left.\begin{aligned} m &= k_E k_2 k_3 \\ h_4 &= M k_3 T_{do}^{'} T_E; h_3 = M\left(k_3 T_{do}^{'} + T_E\right) \\ h_2 &= M + 314 K_1 k_3 T_{do}^{'} T_E + k_E k_6 k_3 M \\ h_1 &= 314 K_1 (k_3 T_{do}^{'} + T_E) - 314 k_2 k_3 k_4 T_E \\ h_0 &= 314(K_1 - k_2 k_3 k_4 - k_E k_2 k_3 k_5 - k_E k_1 k_3 k_6) \end{aligned}\right\} \tag{10}$$

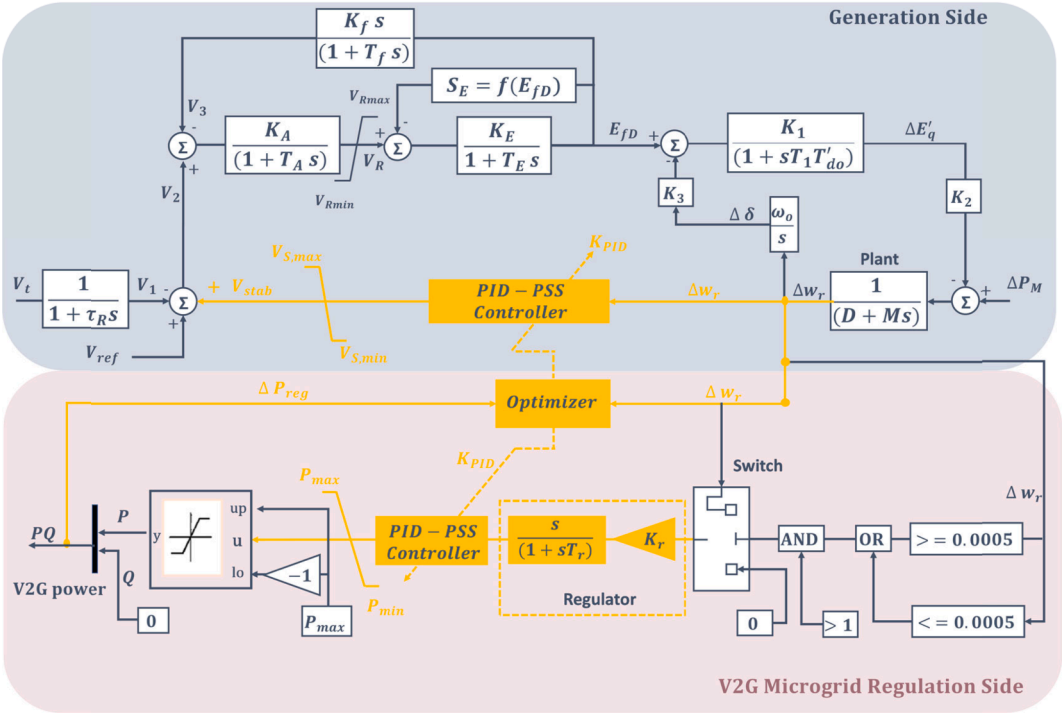

Fig. 6. Linearized model of synchronous machine with the adaptive PID-PSS controller based V2G regulation scheme.

$$G_{OL}(s,m,h)=\frac{-[m_{11},m_{12}]s}{[h_{41},h_{42}]s^4+[h_{31},n_{32}]s^3+[h,n_{22}]s^2+[h_{11},h_{12}]s+[h_{01},h_{02}]} \tag{11}$$

where,

$$h_{i1}=\overbrace{p,Q}^{min}(h_i);$$
$$h_{i2}=\overbrace{p,Q}^{max}(h_i);$$
$$m_{11}=\overbrace{p,Q}^{min}(m);$$
$$m_{12}=\overbrace{p,Q}^{max}(m);$$

$i=0,1,2,3,4$

$$G_{CL}(s,m,h)=\frac{-[m_{11},m_{12}]s}{\begin{array}{l}[h_{41},h_{42}]s^4+[h_{31},h_{32}]s^3+[h_{21}+m_{11}k_d,h_{22}+m_{21}k_d]s^2+\\ [h_{11}+m_{11}k_p,h_{12}+m_{21}k_p]s+[h_{01}+m_{11}k_i,h_{02}+m_{12}k_i]\end{array}} \tag{12}$$

It is seen from [38] that the values of these coefficients depend mainly on the nominal inertia of the synchronous machine and time constants. Furthermore, they differ over time due to variation in loads intermittently, so the coefficient's maximum values are determined according to changes in active and reactive power (P and Q). Thus, the transfer function, in this case, can be expressed in Eq. (11).

In most cases, the open-loop system is unstable, hence, there is a need to add and design a robust PSS-based PID to mitigate these issues. With the addition of the PID-PSS, which is adaptively tuned by the HHO optimizer, the system converted into a closed-loop one as shown in Fig. 5, and the final transfer function for the proposed system $G_{CL}(s,m,h)$ can be described as follows:

It is noted from Eq. (12) that the system order is four, so the denominator needs to be factorized (with high order) to a second order using an m-file code as:
then finding the poles and zeros as:

$$sys=tf\big(-[m_{11},m_{12}],\ [h_{41},h_{42}]\ [h_{31},h_{32}]\ [h_{21}+m_{11}k_d,h_{22}+m_{21}k_d]\ \big[h_{11}+m_{11}k_p,h_{12}+m_{21}k_p\big]\ \ [h_{01}+m_{11}k_i,h_{02}+m_{12}k_i]\big)$$

poles = roots(cell2mat(sys, Den))

zeros = roots(cell2mat(sys, Num))

So, it will be easier to determine the parameters indices using the standard formula as follows:

$$T.F=\frac{\omega_n^2}{s^2+2\zeta\omega_n s+\omega_n^2} \tag{13}$$

$$\left.\begin{array}{c}T_s=\dfrac{4}{\omega_n\zeta}\\ M_P=e^{\left(\frac{-\pi\zeta}{\sqrt{(1-\zeta^2)}}\right)}\\ E_{ss}=\lim\limits_{s\to0}sE(s)=\lim\limits_{s\to0}s\left(\dfrac{\Delta V_{ref}(s)}{G_{CL}(s,m,n)}\right)\end{array}\right\} \tag{14}$$

In this study, PID gains are adjusted using the direct adaptive HHO optimizer that can robustly stabilize the proposed system as well as maintain the gains of the output controller within limits for practical prominence as:

$$k_p^{min}\le k_p\le k_p^{max}$$

$$k_i^{min}\le k_i\le k_i^{max}$$

$$k_d^{min}\le k_d\le k_d^{max}$$

The second suggested approach is to simplify the linearized model in Fig. 6 to get the time response parameters of the feedback second-order system in presence of a PID-PSS controller linked with the automatic voltage regulation AVR. If it is assumed for simplifications that $S_E=0$ and the superposition method as discussed in detail before in [30], the actual transfer function can be represented as:

$$G(s)=\left(\frac{\frac{K_E+K_A}{T_AT_E}}{s^2+\left(\frac{T_AK_E+T_E}{T_AT_E}\right)s+\frac{K_E+K_A}{T_AT_E}}\right)f(V_{stabilizer}) \tag{15}$$

Where, $V_{stabilizer}$ is a function in PID gains as stated in Eq. (7). So,

$$\omega_n=\left(\sqrt{\frac{K_E+K_A}{T_AT_E}}\right)(K_{PID})_{PSS} \tag{16}$$

and

$$\zeta=\frac{T_AK_E+T_E}{2T_AT_E\left(\sqrt{\frac{K_E+K_A}{T_AT_E}}\right)(K_{PID})_{PSS}} \tag{17}$$

then

$$\left.\begin{array}{c}T_s=\dfrac{8(T_AT_E)}{T_AK_E+T_E}\\ M_P=e^{\left(\frac{-\pi^*\frac{T_AK_E+T_E}{2T_AT_E\left(\sqrt{\frac{K_E+K_A}{T_AT_E}}\right)(K_{PID})_{PSS}}}{\sqrt{\left(1-\left(\frac{T_AK_E+T_E}{2T_AT_E\left(\sqrt{\frac{K_E+K_A}{T_AT_E}}\right)(K_{PID})_{PSS}}\right)^2\right)}}\right)}\\ E_{ss}=\lim\limits_{s\to0}s\left(\dfrac{\Delta V_{ref}(s)}{G_{CL}(s,m,n)}\right)\end{array}\right\} \tag{18}$$

As a result, Eqs. (16)-(18) will be used inside the proposed HHO optimizer to calculate the objective function. Moreover, it is noted from

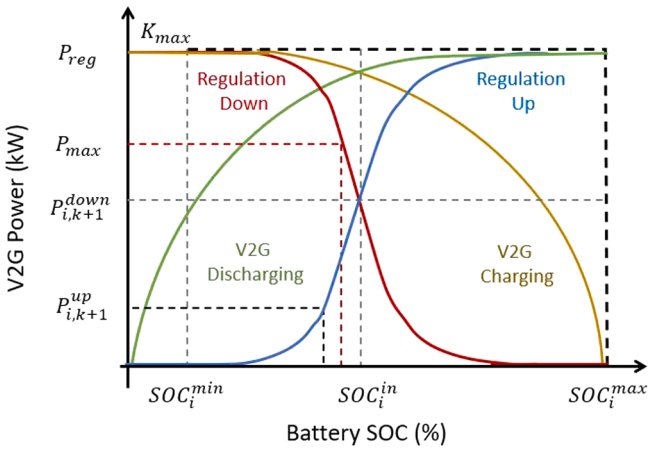

Fig. 7. EVs battery SOC balance control considering V2G power.

Fig. 6 that two input signals are feeding the optimizer from the generation side ($\Delta\omega_r$) and V2G regulation side (P_{reg}) signals as guides for adjusting the gain parameters of the PID-PSS controller.

4.2. Vehicle-to-Grid concept

This work focuses on the contribution of EVs using the V2G inclusion for frequency and voltage regulations for islanded residential MG. The internal power loss and battery technology types are not considered as these hypotheses do not affect the goals of this study. The charging scenario of EVs was concluded in two phases: first, maintain the battery's SOC, and second adjust its energy level. These levels ought to be combined in the determination of the V2G power regulation. In addition, the SOC level was designed around 50 %, which means that the regulation up/down demonstrated a negative SOC-dependent correlation of the battery as stated in Fig. 7, further details in Appendix [39,40].

4.2.1. V2G Integration with islanded residential MG

The incorporation of V2G with the MG makes it easy to use the vehicle's excess battery power to control the MG frequency whenever a sudden event happens during the day. When the demand for loads is low, then solar energy may meet this demand and when the demand increases, the shortage of power will be provided by the diesel generator. All of these are considered to have a charging station at the workplace and at home. The estimated power capacity of all charging stations using 100 EVs is 4 MW (4 kW per EV) [35].

4.2.2. Proposed V2G scheme

The proposed V2G scheme has two missions: it controls the charging of the batteries and the use of the accessible power to regulate the MG at the moment of a sudden event that may happen. The battery's SOC can

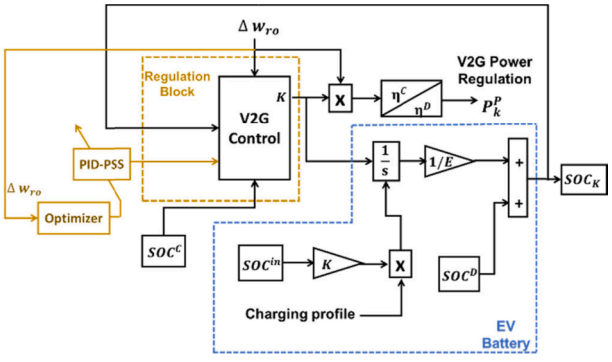

Fig. 8. V2G control-based SOC controller with adaptive PID-PSS.

Table 3
Suggested V2G Initial Parameters.

Parameter	Value
Number of EVs	100
Number of EV aggregations	5
Rated power (MW)	4
Rated capacity (kWh)	85
Regulator proportional gain (K_p)	2
Regulator integral gain (K_i)	$4e^3$
Charging/discharging efficiency	90 %
Plugin/out time	stated in [35]

Table 4
Suggested PID-PSS Parameters.

For generation side	
Stabilizer gain (K_{PSS})	1
Proportional gain (K_p)	
Integral gain (K_i)	Tuned adaptively
Derivative gain (K_D)	
Washout time constant (T_w) in sec	10
Upper Limit ($V_{S,max}$)	0.15
Lower Limit ($V_{S,min}$)	−0.15
For V2G-microgrid regulation side	
Regulator gain (K_r)	$1e^3$
Regulation proportional gain (K_p)	
Regulation integral gain (K_i)	Tuned adaptively
Regulation derivative gain (K_D)	
Regulator time constant (T_r) in sec	25
Upper Limit (P_{max})	$1e^6$
Lower Limit (P_{min})	$1e^{-6}$
PID update frequency	40 Hz

be written as [40]:

$$SOC_{i,k} = SOC^{in}_i + \frac{1}{E^r_i} + \Delta E_i \tag{19}$$

where ΔE_i indicates the battery energy change during the process of discharging/charging and can be given as:

$$\Delta E_i = \int_0^k P_i(k)dk \tag{20}$$

The V2G regulation-based SOC controller supported with direct adaptive PID-PSS was considered free from ramp rate limitations related to traditional generating units, as described in Fig. 8. It was largely due to the advantage of rapid regulation of EVs. The nominal and suggested parameters for V2G with conventional PI and proposed PID-PSS controllers that are used in this work are delineated in Tables 3 and 4.

The conceptual procedures of this work are stated in the flowchart shown in Fig. 9, which two control mechanisms for EVs are identified: MG regulation and charging controllers after observing the residential MG frequency to decide if (G2V) or (V2G) is needed, more details about power regulation and total V2G power required at each EVs charging station are given in Appendix section B.

5. Results and discussion

In this study, the V2G system model is analyzed and simulated using the time domain under a 24 hr scenario taking into account different conditions of operation such as load demand switching and partial shading of solar PV. The aggregated model is comprised of 100 EVs divided into 5 different user profiles, each connected to the MG for regulation purposes. The EVs have a rated capacity of 85 kWh and a rated power of 40 kW per EV, as indicated in Table 5 [35]. Moreover, the number of cars in regulation mode and in charge mode is displayed in

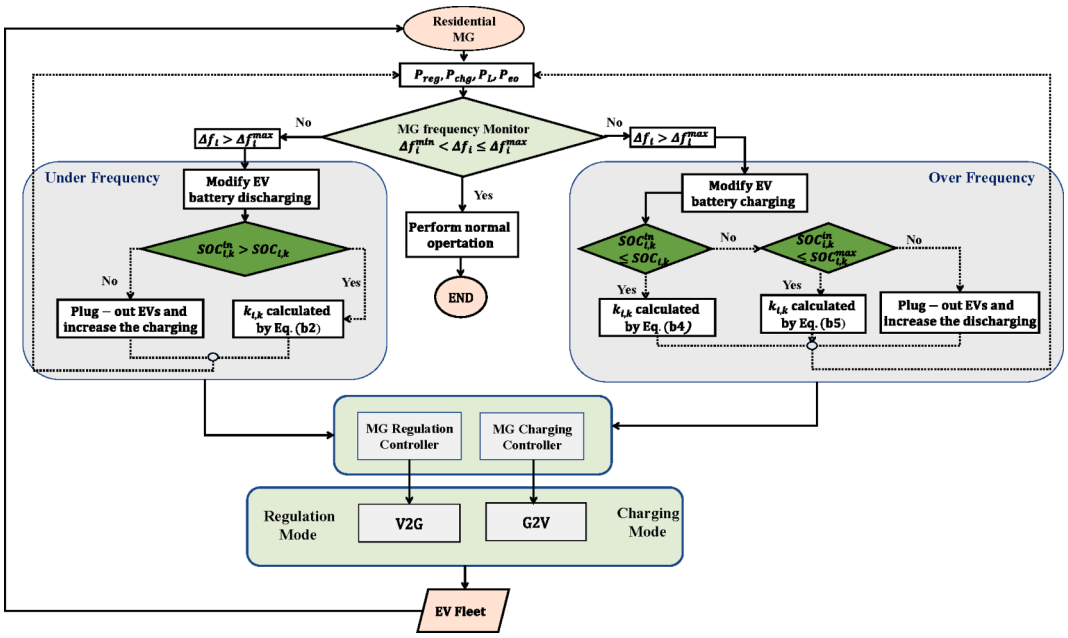

Fig. 9. The main procedures of the proposed strategy.

Table 5
Suggested EVs profiles.

Profiles	Status	% Of EVs
#1	Users working from 8 to 4 pm with a 2 hr driving to work from home and 2 hr vice versa. Available charger station at the workplace.	35 %
#2	Users working from 8 to 4 pm with a 2 hr driving to work from home and 2 hr vice versa. No charger station is available at the workplace	25 %
#3	Users working from 8 to 4 pm with a 3 hr driving to work from home and 3 hr vice versa. Available charger station at the workplace.	10 %
#4	Users don't use their EVs and are connected to the MG for 24 hr.	20 %
#5	Users working from 20 pm to 4 am with 2 hr driving to work from home and 2 hr vice versa. No charger station is available at the workplace.	10 %

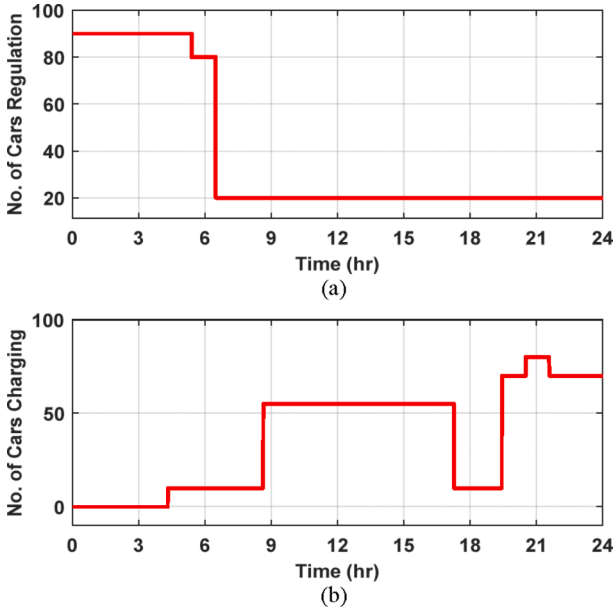

Fig. 10. Number of cars in a) regulation mode, and b) charging mode.

Fig. 10.

The nominal MG parameters including the governor, SG, transformer, excitation system, and loads are stated in subsection (A) of the Appendix part. The effectiveness and robustness of the proposed control strategy combining V2G with an adaptive PID-PSS was evaluated by testing the residential islanded MG system in two scenarios. The results were then compared to those of a conventional system-based PI-controller, both with and without the inclusion of V2G, in the absence of PSS, all located on the microgrid regulation side.

Case 1: performance assessment under load demand switching

In this case, on the generation side, the studied MG system using the V2G scheme with adaptive PID-PSS controller has been examined under the effect of a 3 MW load disconnection at t = 40 *sec* with disconnected solar PV. As a result, the load disconnection will lead to an unexpected variation in power provided from sources and demand loads resulting in oscillations in MG voltage and frequency.

Fig. 11a-11e display the SG output in terms of voltage, frequency, electrical and mechanical power for the conventional residential MG system using conventional PI-controller with and without V2G scheme (no PSS), as well as the proposed V2G scheme with the adaptive PID-PSS controller. It has to be emphasized that no V2G implies that the EVs are only connected as loads, whereas no PSS means that the PSS is connected only on the generation side, conventionally (excitation system). It is clear from Fig. 11a that the MG frequency for the proposed scheme starts to stabilize after 2 *sec* from switching off the load at t = 40 *sec* and deviates by (±0.06 Hz). On the hand, the conventional system (no PSS and no V2G) takes about 10 *sec* to settle and oscillates by ± 0.006 pu (±0.34 Hz), system with only V2G without PSS deviates by ± 0.0022 pu (±0.14 Hz), which remains for 5 *sec* to be settled. It is observed from Fig. 11b and 11c that the proposed scheme needs more time about 7.68 *sec* to match the power reference with fewer deviations compared to the other schemes. Regarding the voltage, as shown in Fig. 11d and 11e, the voltage for the proposed scheme begins to stabilize at 2.2 *sec* and deviates by 0.006 pu during triggering the load. On the other hand, the conventional system (no PSS and V2G) includes higher oscillations by

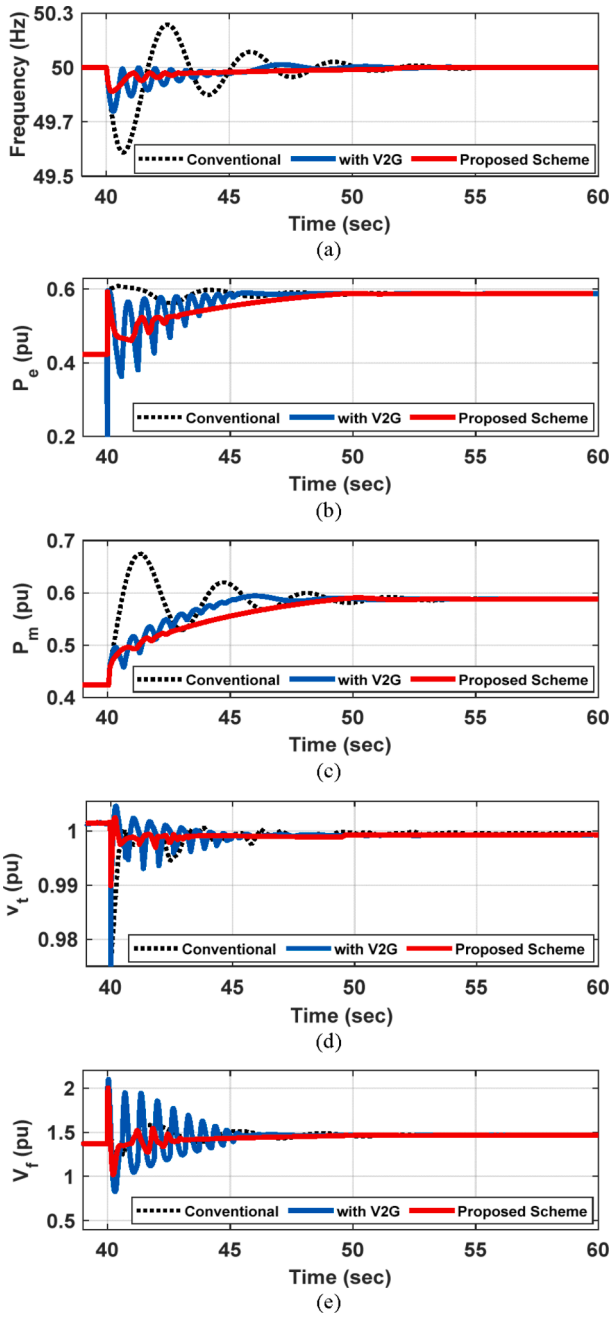

Fig. 11. Diesel generator responses: a) frequency, b) output power, c) mechanical power, d) terminal voltage, and e) excitation field voltage.

0.118 pu that remains 10 *sec* and 0.112 pu that remains for 5 *sec* to stabilize for system with V2G (no PSS). The final results in Fig. 11a-d indicate that the system equipped with PSS in both V2G MG regulation and generation sides provides superior performance with a greater reduction in oscillations that occurred within the MG during load disconnection in terms of (T_s, M_p, E_{ss})through the defined objective function in Eq. (8).

From the load side, Fig. 12 shows the dynamic residential load responses including terminal voltage, current, active power, and reactive power. With the proposed scheme, the load demand responses are different compared to the system with disabled V2G and PSS. It is seen from Fig. 12a that there is a drop in voltage due to switching the load at t = 40 *sec*, which decreased by 16.55 V for the conventional system, 21.86 V for the system with only V2G (no PSS), and 13.65 V for the proposed scheme. After the event occurred, the studied systems try to

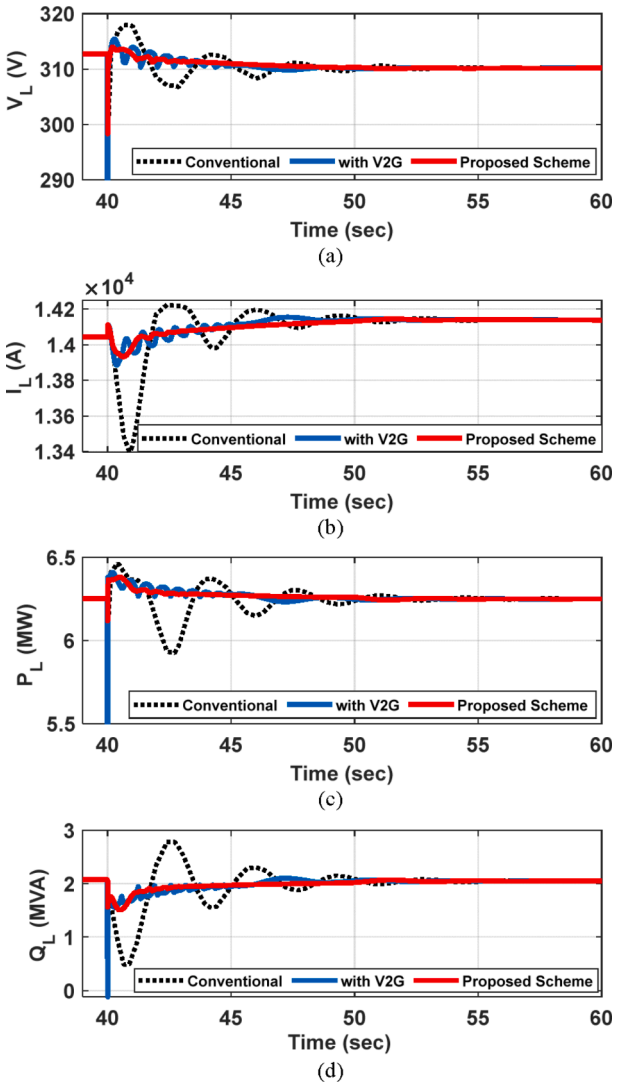

Fig. 12. Residential load responses: a) Voltage, b) current, c) active, d) and reactive power.

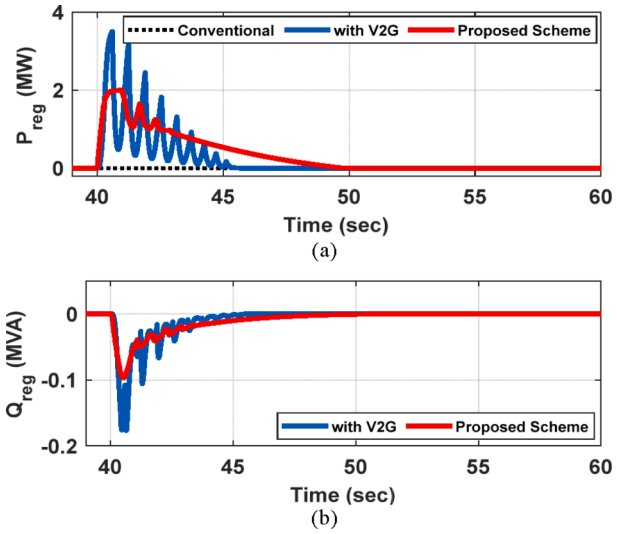

Fig. 13. V2G power regulation.

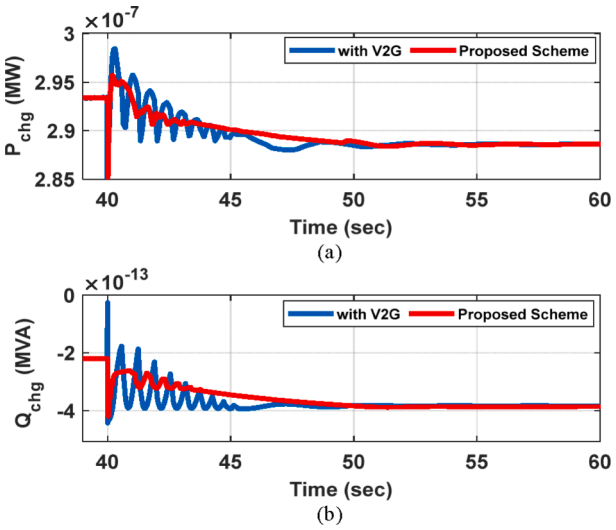

Fig. 14. V2G Charging power.

recover and back again to the nominal value. These are accompanied by oscillations reaching ± 6 V for the conventional system, ± 2.8 V for the system with only V2G (no PSS), and ± 1.05 V for the proposed scheme, which is considered a good indication for using the PSS with V2G at the MG regulation side. Fig. 12b exhibits the amount of drawn current during the switching moment of load.

The current during switching the load off decreased by 0.113 kA, 0.159 kA, and 0.646 kA for the proposed scheme, the system with only V2G (no PSS), and system without both V2G and PSS, respectively, as compared to the previous occurrence of the triggering. It can be seen from Fig. 12b that the amount of oscillation in the current is low in case of the proposed scheme compared to the other ones. The main reason behind this is the use of an adaptive PID-PSS controller at the MG regulation side with V2G that reduced power consumption and limited voltage drop in the MG. Furthermore, it enhanced the performance of the residential MG by providing smoother and faster response than the other schemes after 2.84 *sec* from the switching period.

It is observed from Fig. 12c-12d that the amount of power before disconnecting the load is 6.253 MW and 2.08 MVAR. During switching the load off, the load power dipped, and oscillations varied from 0.465 MW, 0.409 MW, and 0.361 MW for the conventional system, system with only V2G (no PSS), and proposed scheme, respectively. Furthermore, from Fig. 12c, the load power reached the predefined value at different times by 52.15 *sec* for the conventional system, 48.36 *sec* for the system with only V2G (no PSS), and 41.96 *sec* for the proposed scheme. It is seen from Fig. 12d that the amount of $Q_L$decreases during the switching time by 0.52 MVAR for the proposed scheme compared to 1.60 MVAR for the conventional scheme.

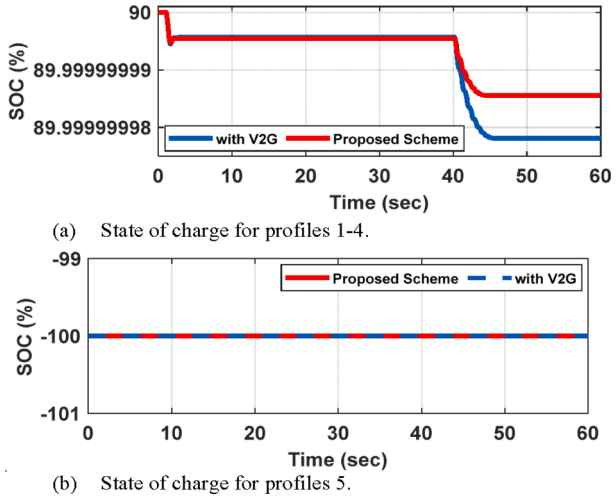

Fig. 15. State of charge for profiles 1–5 for scenario 1.

Moreover, Figs. 13 and 14 show the V2G active and reactive power regulation and charging scenarios under the effect of load disconnection on power-sharing. Negative values refer to the power that EVs provide to the MG. The number of oscillations in Fig. 13a-b and Fig. 14a-b are lower and remain for 2.15 *sec*, when using the PSS with V2G at the MG regulation side compared to the system linked only with V2G without PSS, which stays for 5 *sec* until being smooth. From Figs. 12-14, it is seen that the proposed control strategy using adaptive PID-PSS with the V2G for regulation purposes helped the residential MG system to reduce the oscillations that happen in voltage, current, active power, reactive power, and also for charging and regulation power provided to the studied system during charging periods as compared to other schemes.

Fig. 15 shows the SOC level of each EV profile considered for study. Negative SOC values mean that the cars are still on the road and are not connected for charging. The initial SOC for units 1–4 is 90 %, and 0 % for unit 5. It is seen from Fig. 15 that the discharge amount in EV batteries is less for the proposed scheme than the conventional scheme, so there is still more power available in the batteries after the load disconnection occurs. The main reason behind this is due to the high regulating capacity carried out by adding the PSS on the regulation side resulting in improving the terminal voltage, which has a direct effect on the output power of the diesel generator, thus the power losses are reduced, and more power remains in the batteries for regulation achieved.

This amount of discharge power affects the voltage and frequency of the proposed residential MG. Therefore, with the help of the proposed control strategy, the batteries need to charge less power to reach the predefined SOC level at 90 % as shown in Fig. 15a compared to the conventional one. At the moment of triggering the load, EVs draw power from the MG rather than providing power which leads to voltage and frequency deviations.

Fig. 16a and 16b demonstrate the output tuned control signals of the PID gains-based PSS with the excitation system on the generation side and with V2G on the MG regulation side. A total of 20 iterations with 5 candidate solutions are performed using the HHO optimizer to obtain the optimal solution for the desired function stated in Eq. (8). It is noticed from Fig. 16a-b that the optimizer can sense the change that happens due to disconnecting the load demand at t = 40 *sec*. According to the input rotor speed signal that comes from the SG, the optimizer performs some calculations internally and provide adjusted signals to the PID controller to minimize the error between the measured and reference values (i.e., 50 Hz).

Case 2: Microgrid frequency regulation under a partial shading of solar PV plant.

The performance of the islanded MG under the proposed V2G-based direct adaptive PSS has been tested in the case of partial shading of the solar PV plant at 13 hr (afternoon) to analyze the role of the V2G system in regulating the power and frequency.

The partial shading event is scheduled at 13hr and continues for 5 min. As mentioned in *Case 1*, a change in power between the generation and load demand would occur due to these abrupt events resulting in deviations in the MG frequency. The impact of the partial shading event on the power-sharing by the proposed V2G system to regulate the MG frequency is depicted in Fig. 17. Here, the negative values refer to the power that EVs provide to the MG.

Partial shading of the solar PV is supposed to occur in the afternoon at 13 hr for a time duration of 5 min, then it again starts generating power until it reaches its full capacity as shown in Fig. 17a. Due to the drop in power, the frequency is directly affected where it changed from 49.79 Hz to 50.23 Hz for conventional MG (no V2G and no PSS), from 49.89 Hz to 50.12 Hz for MG-based V2G (no PSS) and varies from 49.93

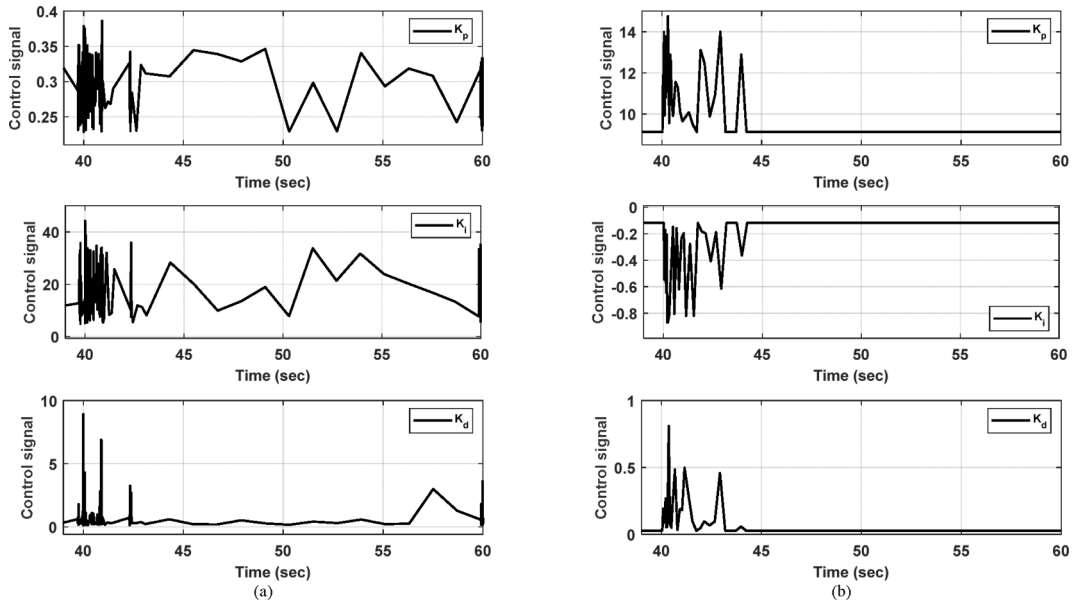

Fig. 16. Control output signal gains of adaptive PID-based PSS with (a) Generation side, (b) V2G regulation side.

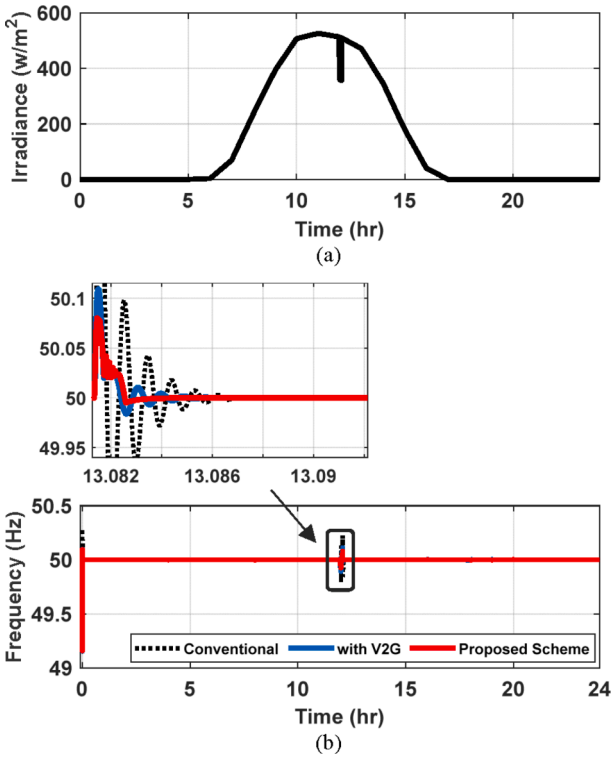

Fig. 17. a) Solar Irradiance, b) MG system frequency response in case of partial shading of PV plant.

Table 6
Comparison of different V2G scenarios.

Case study	Period	Mode	f_{min} (Hz)	f_{max} (Hz)
(1)	t = 0 sec	Conventional	49.14	50.31
		With V2G	49.16	50.12
		Proposed Scheme	49.32	50.01
	t = 40 sec	Conventional	49.58	50.22
		with V2G	49.77	50.02
		Proposed Scheme	49.88	50.00
(2)	t = 0 hr	Conventional	49.14	50.29
		With V2G	49.15	50.11
		Proposed Scheme	49.18	50.08
	t = 13 hr	Conventional	49.79	50.23
		with V2G	49.89	50.12
		Proposed Scheme	49.93	50.07

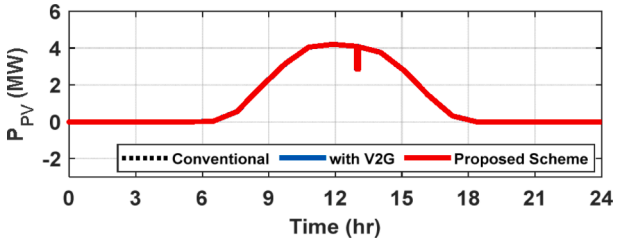

Fig. 18. Active power response of the considered solar PV system.

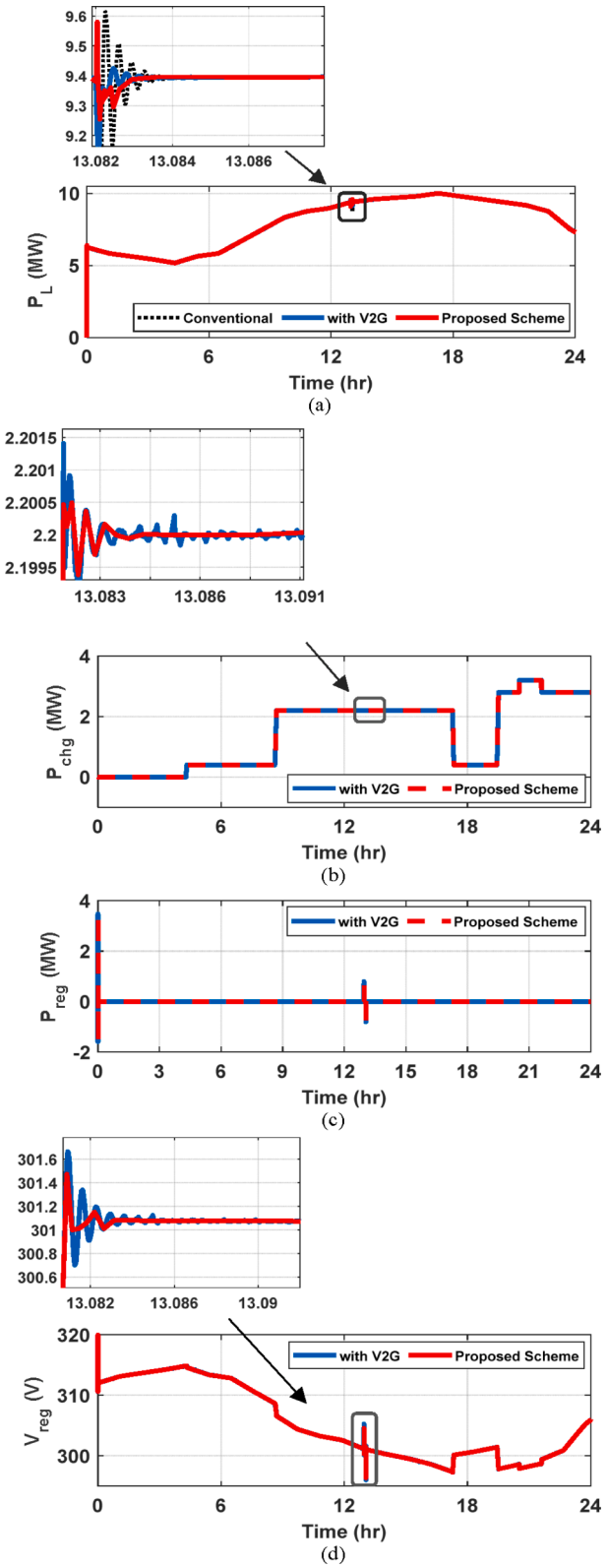

Fig. 19. Residential load power and V2G power regulation and charging.

Hz to 50.07 Hz using the proposed control strategy, as shown in Fig. 17b.

A brief analysis of the deviation in frequency for *Case 1* and *Case 2* is given in Table 6. From Table 6, the maximum and minimum frequency values are presented for each study case. For *Case 1*, the deviation in frequency Δf_{min} is $\pm$ 0.05 Hz for the proposed scheme during switching the load off at t = 40 *sec* compared to other schemes, whose deviation

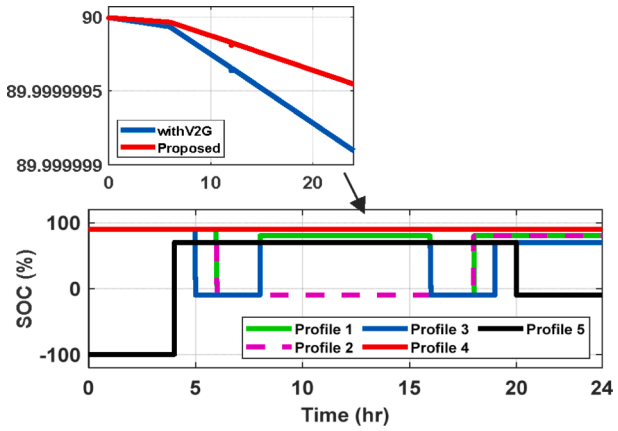

Fig. 20. State of charge for profiles 1–5 for scenario 2.

varies between $\pm$ 0.59 Hz which leads to instability of the MG system if not well controlled. On the other hand, for partial shading event in *Case 2*, it is observed from Table 6 that the deviation in frequency in case of the proposed scheme is less than the conventional system with/without V2G by 0.53 Hz.

Fig. 18 describes the active power of the solar PV system. The peak power obtained from the PV plant at mid-day is 4.21 MW. The power generated from the solar PV plant due to the partial shading effect decreased by 1.84 MW and this dip remained for 5 min, then the solar PV plant begins generating power to its full capacity, as shown in Fig. 18.

Fig. 19 indicates the residential load power, V2G power regulation, and charging scenarios under the effect of the proposed abrupt event (partial shading) on the power-sharing. The negative values refer to the power that EVs provide to the MG. This partial shading will reduce the PV power contribution and for this reason, the proposed scheme using the inclusion of a PID-PSS controller with the V2G will start to supply 0.798 MW from EVs using the V2G concept to regulate the frequency of the considered islanded residential MG during shading moment. On the other hand, if the inclusion of V2G is disabled, EVs will be in charging mode, which behave as loads without regulation of the residential MG. This means that the amount of power consumed by the loads increased as shown in Fig. 19a, and also the charging power increased due to the charging of EVs at this time as shown in Fig. 19b. When the V2G mode is enabled, it is seen that the regulation power is increased by 0.798 MW at t = 13 hr, as shown in Fig. 19c. As a result of providing power to the MG in terms of active and reactive power by EVs, an enhancement is noticed in the MG voltage as shown in Fig. 19d. From Fig. 19a-d, it is observed that fewer flickers using the proposed scheme are present at the moment of PV partial shading, which accounts for improved power quality. These spikes adversely affect the system stability if they are not controlled in a prompt manner. Finally, the percentage of SOC for all suggested EV profiles is shown in Fig. 20 and the negative values of SOC mean that the cars are still on the road and not plugged in for charging.

Fig. 21 shows the output control signal of the PID gains-based PSS that was implemented on the V2G microgrid regulation side. The same nominal parameters of the proposed optimizer as discussed in *Case 1* were used to obtain the fitting value according to the objective function defined in Eq. (8). The optimizer will monitor the change in the rotor speed signal as input (frequency) and then according to the deviation in this signal, the optimizer will perform orders to achieve the function in Eq. (8) and provide tuned signals to the PID controller to minimize the frequency and voltage deviations. Therefore, it is noticeable from Fig. 21 that the optimizer can sense and track the change that happens in the residential MG system during partial shading of the solar PV plant at t = 13 hr (afternoon). Compared to *Case 1*, there are a lot of adjustments made by the optimizer due to the increased time remaining for the suggested shading of the solar PV plant and this is another indication of the optimizer's traceability.

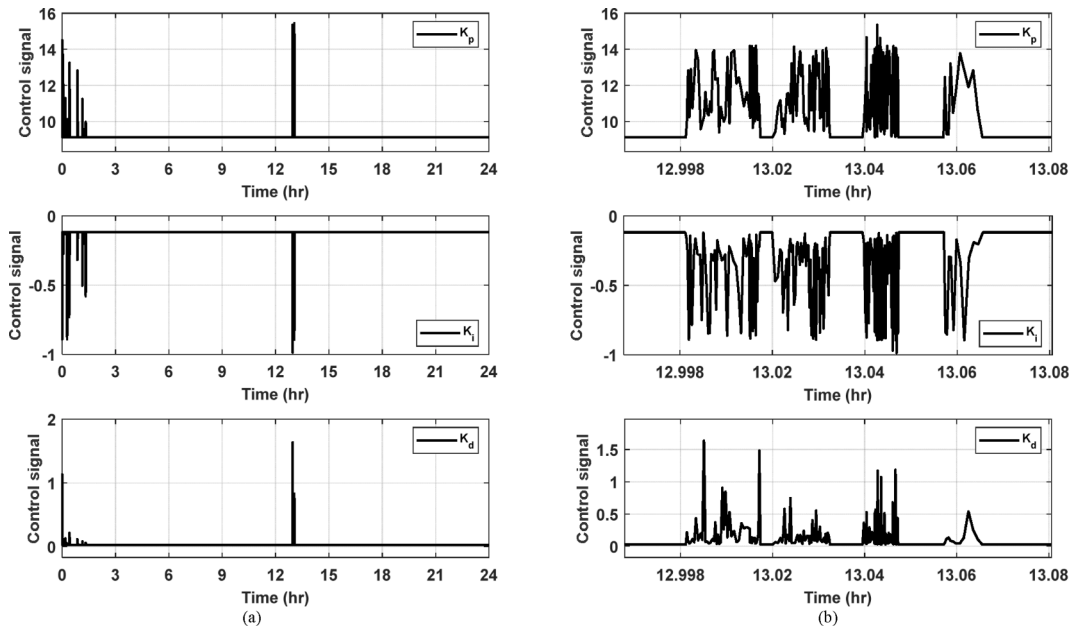

Fig. 21. (a) Output control signal of the adaptive PID-PSS for the V2G regulation side under the effect of solar PV shading at 13 hr. (b) a zoomed in view.

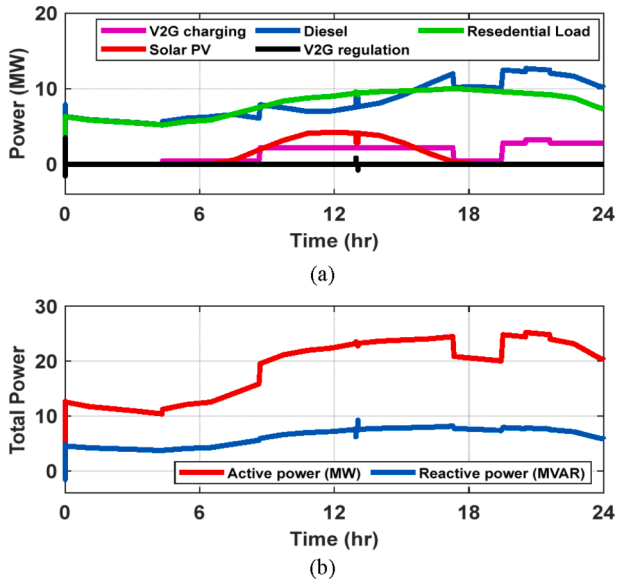

Fig. 22. MG output power by sources (a)Output power per source, (b) Total output active and reactive power.

Table 7
Maximum power by sources.

Types of sources	Value (MW)	Period (hr)
Diesel	12.65	20.01
Solar PV	4.21	12
Residential Load	10	16.99
V2G regulation	0.798	13
V2G charging	3.2	20.01

Fig. 22a shows the output power for all MG sources in this study and are concluded in Fig. 22b in the form of total active and reactive power. It is observed from Fig. 22a that the regulation power increased by 0.798 MW, solar PV power decreased due to shading by 1.22 MW, change in charging power at the beginning of partial shading is 0.013 MW, change in load about 0.19 MW, and finally the amount of diesel power is increased by 2.2 MW at t = 13 hr. The maximum power generated and consumed by each source is stated in Table 7. It is observed that when the partial shading occurs at 13 hr for 5 min, the output power obtained from the PV plant decreased, and the diesel generator contributes to supply additional power to meet the load demand.

6. Conclusion

The key reasons behind the fluctuations caused in power supply, frequency, and voltage within a residential islanded MG, in the presence of partial shading of solar PV plant and switched load demand, are analyzed in this work. The control methods for V2G available in the literature are not well damped, which adversely affects the MG dynamic response. Moreover, they are not well coordinated, complex and suffer from a high computational burden. Therefore, this paper proposed a novel control scheme for frequency, voltage regulation and power-sharing in an islanded residential MG which is mainly powered by the PV power plant along with a diesel generator using the inclusion of V2G scheme. A PID-PSS controller was developed in a direct adaptive manner using the HHO optimizer for the V2G microgrid control side and an excitation system at the generation side to provide a complementary signal for modifying the instability of the faster oscillating MG. The benefit of adding PSS is due to its output boundaries to reduce the degree of terminal voltage fluctuation through transient situations to enrich the dynamic stability performance of the studied residential MG system.

The proposed scheme has been examined under two different scenarios using five different EV profiles versus the conventional system without both V2G and PSS, and with the system with only V2G (no PSS). It has been demonstrated that the addition of an adaptive PID-PSS controller provides a significant improved frequency and voltage qualities in case of switching the load demand off and partial shading of PV plant, where the deviations in frequency and voltage were fewer than the conventional system (no PSS and no V2G) and the system with only V2G (no PSS). Also, the proposed control strategy start stabilizes faster than the other ones with less steady state error. The final findings confirmed that the proposed control scheme can be effectively implemented in the studied islanded residential MGs system and positively contributes towards the deviations in frequency, voltage, and regulate the power shared by V2G with good dynamic performance.

For the future perspective study, it is envisaged that the proposed

control scheme using adaptive PID-PSS in the V2G microgrid regulation side would be applied and tested on a multi-bus power system.

CRediT authorship contribution statement

Hussein Abubakr: Conceptualization, Software, Validation, Methodology, Writing – original draft. **Abderezak Lashab:** Visualization, Data curation, Writing – review & editing. **Juan C. Vasquez:** Supervision, Writing – review & editing. **Tarek Hassan Mohamed:** Formal analysis, Investigation. **Josep M. Guerrero:** Supervision, Funding acquisition.

Declaration of Competing Interest

The authors declare that they have no known competing financial interests or personal relationships that could have appeared to influence the work reported in this paper.

Data availability

No data was used for the research described in the article.

Acknowledgment

Hussein Abubakr is fully funded by the Ministry of Higher Education of the Arab Republic of Egypt; This work is also supported by VILLUM FONDEN under the VILLUM Investigator Grant (no. 25920): Center for Research on Microgrids (CROM);

Appendix

A. A single machine based on synchronous generator parameter [37]:

a) Diesel Engine Governor		
Regulator gain [K()]	29	
Regulator time constants [T_1, T_2, T_3] (sec)	[0.01, 0.02, 0.2]	
Actuator time constants [T_4, T_5, T_6] (sec)	[0.25, 0.009, 0.0384]	
Torque limits [T_{min}, T_{max}]	[0.1, 1]	
Engine time delay T_d (sec)	0.024	
Initial mechanical power (pu)	0.00734	
b) Synchronous generator		
Nominal power (VA), line-to-line voltage (V), and frequency (Hz)	[$15e^6$,$13.8e^3$, 50]	
Stator [R_s](pu)	[0.003]	
Inertia coefficient, friction factor, poles [H(s)F(pu), p()]	[3.7 0 1]	
d) Three-phase Transformer		
Nominal power and frequency [P_n(MW), f_n(Hz)]	[20, 50]	
Winding 1 parameters [V_{1Ph-Ph}(rms), R_1(pu), L_1(pu)]	[$13.8e^3$, 0.002, 0.08]	
Winding 2 parameters [V_{2Ph-Ph}(rms), R_2(pu), L_2(pu)]	[400, 0.002, 0.08].	
Magnetizing resistance R_m(pu)	500	
Magnetizing inductance L_m(pu)	500	
e) Excitation system		
Low-pass filter time constant T_r	$20e^{-3}$	
Regulators gain and time constant [K_a(), T_a]	[300, 0.001]	
Exciter gain and time constant [K_e(), T_e]	[1, $1e^{-3}$]	
Damping filter gain and time constant [K_f(), T_f]	[0.001, 0.1]	
initial values of terminal voltage and field voltage [V_{to} (pu) ,V_f (pu)]	[1, 1.0072]	
Regulator output limits and gain [E_{Fmin} (),E_{Fmax}, K_p()]	[-11.5, 11.5, 0].	
c) Demand loads	Type	
load 1	Resistive	3 MW
load 2	Residential	10 MW with 0.95 PF

B. Determination of the V2G power regulation [22]

$$\begin{cases} P_{j,k+1}^{up,1} = \sum_{i=1}^{N_j^1} \left(P_{max} k_{i,k}^{up} \right) \\ P_{j,k+1}^{down,1} = \sum_{i=1}^{N_j^1} \left(P_{max} k_{i,k}^{down} \right) \end{cases} \quad \text{(b1)}$$

where $k_{i,k}^{up}$ and $k_{i,k}^{down}$ are the regulation up (discharging) and down (charging) droops of i^{th} EV at time k and calculated as follows:

If $SOC_{i,k} \leq SOC_i^{min}$

$$\begin{cases} k_{i,k}^{up} = 0 \\ k_{i,k}^{down} = 1 \end{cases} \tag{b2}$$

where the values [0, 1] are represented the K_{max}.

If $SOC_{i,k} \geq SOC_i^{max}$

$$\begin{cases} k_{i,k}^{up} = 1 \\ k_{i,k}^{down} = 0 \end{cases} \tag{b3}$$

If $SOC_i^{min} < SOC_{i,k} \leq SOC_i^{in}$

$$\begin{cases} k_{i,k}^{up} = 0.5\left(1 - \sqrt{\dfrac{SOC_{i,k} - SOC_i^{in}}{SOC_i^{min} - SOC_i^{in}}}\right) \\ k_{i,k}^{down} = 0.5\left(1 + \sqrt{\dfrac{SOC_{i,k} - SOC_i^{in}}{SOC_i^{min} - SOC_i^{in}}}\right) \end{cases} \tag{b4}$$

If $SOC_i^{in} < SOC_{i,k} \leq SOC_i^{max}$

$$\begin{cases} k_{i,k}^{up} = 0.5\left(1 + \sqrt{\dfrac{SOC_{i,k} - SOC_i^{in}}{SOC_i^{max} - SOC_i^{in}}}\right) \\ k_{i,k}^{down} = 0.5\left(1 - \sqrt{\dfrac{SOC_{i,k} - SOC_i^{in}}{SOC_i^{max} - SOC_i^{in}}}\right) \end{cases} \tag{b5}$$

where SOC_i^{max},SOC_i^{min},$SOC_{i,k}$are the maximum, minimum, and initial state of the ith EV charge at time k. The correlation between EVs and V2G power is given as:

$$P_{max} = P_{j,k+1}^{up,1} + P_{j,k+1}^{down,1} \tag{b6}$$

The total V2G power required at each EVs charging station can be calculated as follows:

$$\begin{cases} P_{j,k+1}^{up} = P_{j,k+1}^{up,1} + P_{j,k+1}^{up,2} + \cdots \\ P_{j,k+1}^{down} = P_{j,k+1}^{down,1} + P_{j,k+1}^{down,2} + \cdots \end{cases} \tag{b7}$$

$\boldsymbol{j} = 1, \cdots . \boldsymbol{p}$

The total V2G power including the power uploaded by CSO is defined as follows:

$$\begin{cases} P_{j,k+1}^{up,1} = \sum_{j=1}^{p}\left(P_{i,k+1}^{up}\right) \\ P_{j,k+1}^{down,1} = \sum_{j=1}^{p}\left(P_{i,k+1}^{down}\right) \end{cases} \tag{b8}$$

References

[1] Abubakr H, Vasquez JC, Mahmoud K, Darwish MMF, Guerrero JM. Comprehensive Review on Renewable Energy Sources in Egypt—Current Status, Grid Codes and Future Vision. IEEE Access 2022;10:4081–101.

[2] European Environment Agency, Electric vehicles in Europe: EEA report no. 20. Publications Office of the EU, 2016, https://data.europa.eu/doi/10.2800/100230.

[3] Cheng Y, Zhang N, Zhang B, Kang C, Xi W, Feng M. Low-Carbon Operation of Multiple Energy Systems Based on Energy- Carbon Integrated Prices. IEEE Trans Smart Grid March 2020;11(2):1307–18.

[4] Bibak B, Tekiner-Moğulkoç H. A comprehensive analysis of Vehicle to Grid (V2G) systems and scholarly literature on the application of such systems. Renewable Energy Focus 2021;36:1–20.

[5] Rajaeifar MA, Ghadimi P, Raugei M, Wu Y, Heidrich O. Challenges and recent developments in supply and value chains of electric vehicle batteries: A sustainability perspective. Resour Conserv Recycl 2022;180:106144.

[6] Gschwendtner C, Sinsel SR, Stephan A. Vehicle-to-X (V2X) implementation: An overview of predominate trial configurations and technical, social and regulatory challenges. Renew Sustain Energy Rev 2021;145:110977.

[7] Liu H, Hu Z, Song Y, Wang J, Xie X. Vehicle-to-grid control for supplementary frequency regulation considering charging demands. IEEE Trans Power Syst 2014; 30:3110–9.

[8] Bayati M, Abedi M, Gharehpetian GB, Farahmandrad M. Short-term interaction between electric vehicles and microgrid in decentralized vehicle-to-grid control methods. Prot Control Mod Power Syst 2019;4:1–11.

[9] Meng J, Mu Y, Jia H, Wu J, Yu X, Qu B. Dynamic frequency response from electric vehicles considering travelling behavior in the Great Britain power system. Appl Energy 2016;162:966–79.

[10] Yilmaz M, Krein PT. Review of the impact of vehicle-to-grid technologies on distribution systems and utility interfaces. IEEE Trans Power Electron 2013;28(12 Dec).

[11] Nour M, Chaves-Ávila JP, Magdy G, Sánchez-Miralles Á. Review of positive and negative impacts of electric vehicles charging on electric power systems. Energies 2020;13(18):4675.

[12] Shrimali B, Maherchandani JK, Chhipa AA. Vehicle to Grid System Integration for Frequency Regulation of Renewable Based Microgrid. In 2021 International Conference on Sustainable Energy and Future Electric Transportation (SEFET), IEEE, pp. 1-6, Jan. 2021.

[13] Alsharif A, Tan CW, Ayop R, Dobi A, Lau KY. A comprehensive review of energy management strategy in Vehicle-to-Grid technology integrated with renewable energy sources. Sustain Energy Technol Assess 2021;47:101439.

[14] Iqbal S, Xin A, Jan MU, Abdelbaky MA, Rehman HU, Salman S, et al. Aggregation of EVs for primary frequency control of an industrial microgrid by implementing grid regulation & charger controller. IEEE Access 2020;8:141977–89.

[15] Cundeva S, Dimovski A. Vehicle-to-grid system used to regulate the frequency of a microgrid. In IEEE EUROCON 2017-17th International Conference on Smart Technologies, IEEE; 2017, p. 456-460.

[16] Shi R, Li S, Zhang P, Lee KY. Integration of renewable energy sources and electric vehicles in V2G network with adjustable robust optimization. Renew Energy 2020; 153:1067–80.

[17] Acharige SS, Haque ME, Arif MT, Hosseinzadeh N, Saha S. A Solar PV Based Smart EV Charging System with V2G Operation for Grid Support. In 2021 31st Australasian Universities Power Engineering Conference (AUPEC), IEEE, pp. 1-6, Sept. 2021.
[18] Singh B, Verma A, Chandra A, Al-Haddad K. Implementation of Solar PV-Battery and Diesel Generator Based Electric Vehicle Charging Station. IEEE Trans Ind Appl 2020;56(4):4007–16.
[19] Dharmakeerthi CH, Mithulananthan N, Saha TK, Overview of the impacts of plug-in electric vehicles on the power grid, in 2011 IEEE PES Innovative Smart Grid Technologies, pp. 1-8, Nov. 2011.
[20] Han S, Han S, Sezaki K. Estimation of achievable power capacity from plug-in electric vehicles for V2G frequency regulation: Case studies for market participation. IEEE Trans Smart Grid 2011;2(4):632–41.
[21] Abubakr H, Mohamed TH, Hussein MM, Guerrero JM, Agundis-Tinajero G. Adaptive frequency regulation strategy in multi-area microgrids including renewable energy and electric vehicles supported by virtual inertia. Int J Electr Power Energy Syst Jul. 2021;129:106814.
[22] Iqbal S, Xin A, Jan MU, Salman S, Zaki AUM, Rehman HU, et al. V2G strategy for primary frequency control of an industrial microgrid considering the charging station operator. Electronics 2020;9(4):549.
[23] Zhang Q, Li Y, Li C, Li C-Y. Real-time adjustment of load frequency control based on controllable energy of electric vehicles. Trans Inst Meas Control 2020;42:42–54.
[24] Shakerighadi B, Anvari-Moghaddam A, Ebrahimzadeh E, Blaabjerg F, Bak CL. A hierarchical game theoretical approach for energy management of electric vehicles and charging stations in smart grids. IEEE Access 2018;6:67223–34.
[25] Bevrani H, Shokoohi S. An intelligent droop control for simultaneous voltage and frequency regulation in islanded microgrids. IEEE Trans Smart Grid 2013;4:1505–13.
[26] Dahab YA, Abubakr H, Mohamed TH. Adaptive load frequency control of power systems using electro-search optimization supported by the balloon effect. IEEE Access 2020;8:7408–22.
[27] Abubakr H, Guerrero JM, Vasquez JC, Mohamed TH, Mahmoud K, Darwish MM, et al. Adaptive LFC Incorporating Modified Virtual Rotor to Regulate Frequency and Tie-Line Power Flow in Multi-Area Microgrids. IEEE Access 2022;10:33248–68.
[28] Liu H, Qi J, Wang J, Li P, Li C, Wei H. EV dispatch control for supplementary frequency regulation considering the expectation of EV owners. IEEE Trans Smart Grid 2016;9:3763–72.
[29] Ray PK, Paital SR, Mohanty A, Eddy FY, Gooi HB. A robust power system stabilizer for enhancement of stability in power system using adaptive fuzzy sliding mode control. Appl Soft Comput 2018;73:471–81.
[30] Abubakr H, Vasquez JC, Mohamed TH, Guerrero JM. The concept of direct adaptive control for improving voltage and frequency regulation loops in several power system applications. Int J Electr Power Energy Syst 2022;140:108068.
[31] Farhad Z, Ibrahim EKE, Tezcan SS, Safi SJ. A robust PID power system stabilizer design of single machine infinite bus system using firefly algorithm. Gazi University J Sci 2018;31(1):155–72.
[32] Ruglheck S, Wangdee W. Power system stabilizer tuning comparison for WECC standard-based and PSO-based methods. In: In 2016 13th International Conference on Electrical Engineering/Electronics, Computer, Telecommunications, and Information Technology (ECTI-CON). IEEE; 2016. p. 1–6.
[33] Nishi, H., et al. IEEE Smart Grid Vision for Vehicular Technology: 2030 and Beyond, in IEEE Smart Grid Vision for Vehicular Technology: 2030 and beyond, vol., no., pp.1-65, 15 Jan. 2014.
[34] Power to the People: Nissan and ENEL Launch First Smart Grid Trials. Available online: https://europe.nissannews.com/en-GB/releases/release-140287-power-to-the-people-nissan-and-enel-launch-first-smart-grid-trials (accessed on 6 December 2021).
[35] 24-hour Simulation of a Vehicle-to-Grid (V2G) System, MathWorks.
[36] Jan MU, Xin A, Abdelbaky MA, Rehman HU, Iqbal S. Adaptive and fuzzy PI controllers design for frequency regulation of isolated microgrid integrated with electric vehicles. IEEE Access 2020;8:87621–32.
[37] Abubakr H, Vasquez JC, Mahmoud K, Darwish MMF, Guerrero JM, Robust PID-PSS Design for Stability Improvement of Grid-Tied Hydro Turbine Generator, 2021 22nd International Middle East Power Systems Conference (MEPCON); 2021, pp. 607-612.
[38] Vijaya ASVL, Mangipudi, Manyala SKRR. Control constraint-based optimal PID-PSS design for a widespread operating power system using SAR algorithm. Int Trans Electr Energy Syst 2021;31(12).
[39] Mohamed, TH, Abdel-Rahim, AMM. Single area power system voltage and frequency control using V2G scheme. In 2017 Nineteenth International Middle East Power Systems Conference (MEPCON), IEEE, pp. 971-975, Dec. 2017.
[40] Ota Y, Taniguchi H, Nakajima T, Liyanage KM, Baba J, Yokoyama A. Autonomous distributed V2G (vehicle-to-grid) satisfying scheduled charging. IEEE Transactions on Smart Grid 2011;3(1):559–64.